AEM
Journals.ASM.org

Quantification of Tinto River Sediment Microbial Communities: Importance of Sulfate-Reducing Bacteria and Their Role in Attenuating Acid Mine Drainage

Irene Sánchez-Andrea,[a,b] Katrin Knittel,[c] Rudolf Amann,[c] Ricardo Amils,[b,d] and José Luis Sanz[a]

Universidad Autónoma de Madrid, Departamento de Biología Molecular, Madrid, Spain[a]; Centro de Biología Molecular Severo Ochoa, UAM-CSIC, Madrid, Spain[b]; Max Planck Institute for Marine Microbiology, Bremen, Germany[c]; and Centro de Astrobiología (INTA-CSIC), Torrejón de Ardoz, Spain[d]

Tinto River (Huelva, Spain) is a natural acidic rock drainage (ARD) environment produced by the bio-oxidation of metallic sulfides from the Iberian Pyritic Belt. This study quantified the abundance of diverse microbial populations inhabiting ARD-related sediments from two physicochemically contrasting sampling sites (SN and JL dams). Depth profiles of total cell numbers differed greatly between the two sites yet were consistent in decreasing sharply at greater depths. Although catalyzed reporter deposition fluorescence *in situ* hybridization with domain-specific probes showed that *Bacteria* (>98%) dominated over *Archaea* (<2%) at both sites, important differences were detected at the class and genus levels, reflecting differences in pH, redox potential, and heavy metal concentrations. At SN, where the pH and redox potential are similar to that of the water column (pH 2.5 and +400 mV), the most abundant organisms were identified as iron-reducing bacteria: *Acidithiobacillus* spp. and *Acidiphilium* spp., probably related to the higher iron solubility at low pH. At the JL dam, characterized by a banded sediment with higher pH (4.2 to 6.2), more reducing redox potential (−210 mV to 50 mV), and a lower solubility of iron, members of sulfate-reducing genera *Syntrophobacter*, *Desulfosporosinus*, and *Desulfurella* were dominant. The latter was quantified with a newly designed CARD-FISH probe. In layers where sulfate-reducing bacteria were abundant, pH was higher and redox potential and levels of dissolved metals and iron were lower. These results suggest that the attenuation of ARD characteristics is biologically driven by sulfate reducers and the consequent precipitation of metals and iron as sulfides.

The Tinto River is a natural acidic rock drainage (ARD) environment located in the Huelva region, in southwestern Spain. On its way from Peña de Hierro to the Atlantic Ocean, the Tinto River emerges from the core of the Iberian Pyritic Belt (IPB), one of the largest metal sulfide (pyrite, chalcopyrite, etc.) deposits on Earth. When exposed to air and water, the microbiologically enhanced oxidation of sulfides produces waters with low pH (pH 2.3) and high ferric iron (~2 g liter^{-1}) and sulfate (~6 g liter^{-1}) contents along the river course. Low pH and ferric iron levels facilitate metal solubilization; therefore, when these waters come into contact with metallic sulfides, they become highly metalliferous (Cu, ~0.1 g liter^{-1}; Zn, ~0.2 g liter^{-1}) (20).

ARD results in contamination of aquifer, with secondary effects like the death of fish, rodents, and livestock and reduced crop yields (36). These unpleasant consequences have led to efforts to remediate ARD environments (21). Besides the environmental concerns, there are biological, geochemical, and biotechnological reasons to analyze microbial populations in acidic environments and to understand their ecology. In ARD, acidophilic, chemolithotrophic, aerobic *Bacteria* and *Archaea* dissolve metallic sulfides by oxidizing the iron and sulfur components. Products resulting from these oxidation processes can be used as electron acceptors in dissimilatory reduction of ferric iron and sulfate under anaerobic conditions linked to the carbon and nitrogen cycles. So far, only ARD aquifers have been studied intensively (7, 8, 19, 22, 23); in contrast, little is known about the ARD sediments (17, 41).

At the Tinto River, knowledge of the diversity and abundance of benthic microbial populations is limited to a methanogen population study (43) and a description of the microbial ecology of two contrasting sampling sites (the SN and JL dams) (42). In the latter study, an extensive survey of the Tinto River sediment microbiota was performed using two culture-independent approaches: denaturing gradient gel electrophoresis (DGGE) and 16S rRNA gene sequencing. The taxonomic affiliation of the identified *Bacteria* showed a high degree of diversity, falling into 5 different phyla: *Proteobacteria*, *Firmicutes*, *Bacteroidetes*, *Acidobacteria*, and *Actinobacteria*; meanwhile, all the *Archaea* were affiliated with the order *Thermoplasmatales*. Microorganisms involved in the iron (*Acidithiobacillus ferrooxidans*, *Sulfobacillus* spp., and *Ferroplasma* spp.), sulfur (*Desulfurella* spp., *Desulfosporosinus* spp., and *Thermodesulfobium* spp.), and carbon (*Acidiphilium* spp., *Bacillus* spp., *Clostridium* spp., and *Acidobacterium* spp.) cycles were identified. However, the abundance of these groups of organisms was unknown. In this study, the microbial communities of the Tinto River sediments were quantified for the first time and analyzed in relation to the physicochemical properties of the sediments with the objective of identifying the dominant and active organisms thriving in the sediments and inferring the main microbial activities taking place.

MATERIALS AND METHODS

Field site description and sampling. The selected sediments are located in the Tinto River basin (Huelva). Samples were collected from two

Received 15 March 2012 Accepted 13 April 2012
Published ahead of print 27 April 2012
Address correspondence to José Luis Sanz, joseluis.sanz@uam.es.

doi:10.1128/AEM.00848-12

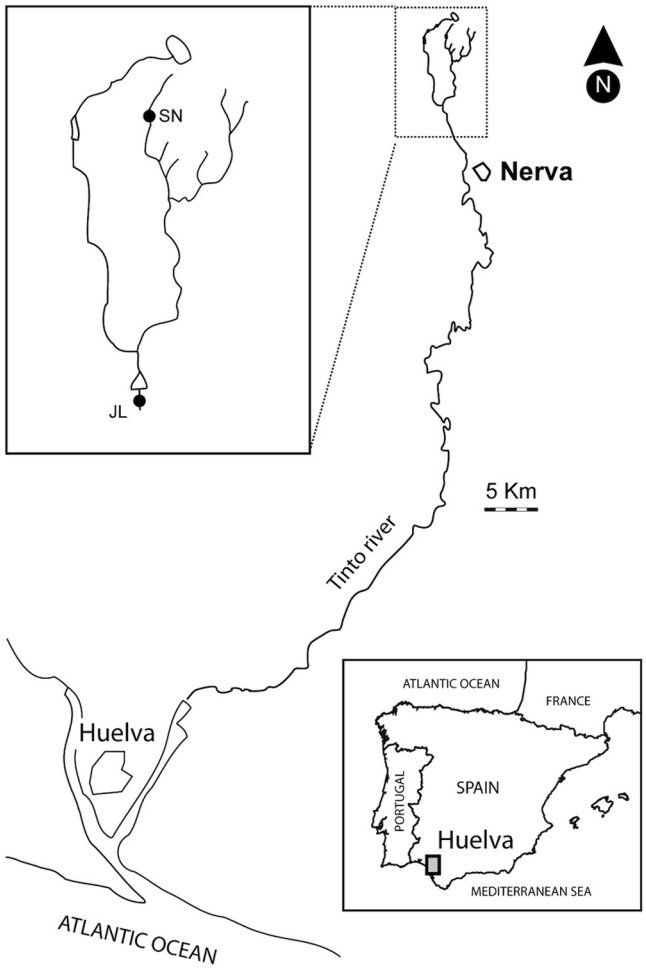

FIG 1 Map of Tinto River in Huelva (Spain) with the location of the studied dams. (Adapted from reference 16a with permission from Elsevier.)

sampling sites (Fig. 1), the SN dam (37.72173°N, 6.557465°W) and the JL dam (37.691207°N, 6.560587°W), at different positions of the river. The SN dam is a spring feeding the main stream of the river, while JL is located in the main course of the river. Sediment cores (inner diameter, 7 cm; length, 45 cm) were taken with a sampler (Eijkelkamp Agrisearch equipment, The Netherlands). The cores were sliced at 5-cm intervals. The redox potential (E) and pH of the drill core samples were measured *in situ* with E and pH probes, connected to a Thermo Orion 290A potentiometer placed into the fresh sediment just after extraction of the core. Sediment samples for hybridization were fixed immediately in 4% (wt/vol) paraformaldehyde (PFA) in phosphate-buffered saline (PBS; 145 mM NaCl, 1.4 mM NaH_2PO_4, 8 mM Na_2HPO_4, pH 7.6) at 4°C for 4 h, washed twice with PBS, and then stored in 50% (vol/vol) ethanol-PBS at −20°C until further use.

Chemical analysis. According to physicochemical parameters and visual appearance, the JL dam core was composed of two main layers, with black and brown colors, whereas the SN core looked homogeneous (Fig. 2a and e). The black (10 to 15 cm) and brown (25 to 30 cm) layers from the JL dam and two layers between 10 to 15 cm and 25 to 30 cm from the SN dam were excised and immediately stored in 15-ml tubes at 4°C until further processing in the laboratory (less than 1 week). Sediments were centrifuged at 13,000 × *g* for 5 min, and the supernatant was analyzed for the presence of heavy metals by inductively coupled plasma mass spectrometry (ICP-MS) and organic anions/volatile fatty acids (VFA) by ionic chromatography (IC) using an 861 Advanced Compact IC instrument. Water samples of both dams were also taken, kept at 4°C, and analyzed by total reflection X-ray fluorescence (TXRF) for S, P, Mn, Fe, Cu, Zn, As, and Ca; by ICP-MS for the rest of the elements; and by thermochemical oxidation (Thermostar LT200 of Hachlange) for total organic carbon (TOC).

Quantification of microorganisms. (i) Sybr green I direct counts. Aliquots of fixed samples were sonicated to detach bacteria from the particles with a sterilized Sonic probe (Bandelin, Sonopuls HD200) for 20 s, 3 times at 20% intensity. Samples were kept on ice for 4 min to precipitate large sediment particles that could clog the filter, and then the supernatant was gently filtered through a black 0.2-μm polycarbonate membrane (Nuclepore; 25-mm diameter) (<0.2 bar). The filters were stained with Sybr green I in Moviol medium as described elsewhere (30). Samples were examined with an epifluorescence microscope (Axioplan 2; Carl Zeiss, Jena, Germany). A minimum of 1,000 Sybr green I-stained cells or at least 100 independent microscopic fields were counted.

(ii) CARD-FISH. Samples were filtered following the same procedure as described above for the direct counts, except that white filters (0.2-μm pore size; Millipore GTTP) were used. *In situ* hybridizations with horseradish peroxidase (HRP)-labeled probes (biomers.net, Ulm, Germany) followed by catalyzed reporter deposition of fluorescently labeled tyramide were carried out as described elsewhere (38). Permeabilization was done with lysozyme (10 mg/ml) for 90 min at 37°C, followed by achromopeptidase (60 U/ml) for Gram-positive cells (44) and proteinase K for *Archaea* (15 μg/ml) (46). Probe sequences and formamide concentrations required for specific hybridization are given in Table 1. Hybridized samples were examined with an epifluorescence microscope (Axioplan 2). For each probe and sample, roughly 1,000 stained cells or at least 100 independent microscopic fields were counted. The signal obtained with probe NON338—a negative control—at each sampling site was subtracted from the specific counts. This signal was about 0.2% of the cell counts for each station.

Total cell numbers in the SN core were too low to allow specific cell counting. Thus, a density gradient centrifugation was carried out to increase the cell density for quantification of less abundant bacterial groups. Cell separation was performed by Histodenz (Sigma-Aldrich) density centrifugation. Subsamples (1 ml) were placed in 2-ml tubes; 1 ml of Hystodenz solution (60% [wt/vol] in PBS, density of 1.3) was carefully placed underneath using a syringe needle to avoid mixing. Centrifugation was performed at 14,000 × *g* for 90 min at 4°C. The supernatant above the Hystodenz layer was treated as explained above for the rest of the samples. Although there was significant cell loss during the procedure (30% compared to untreated samples), this method was shown to maintain representative ratios between communities (48); thus, it could be used for relative counts.

Design, evaluation and application of a *Desulfurella* sp. probe. The high hybridization numbers shown for *Deltaproteobacteria* probe in this study, the abundant presence of *Desulfurella* clones in the former study of Tinto sediments (42), and the lack of a genus-specific probe for *Desulfurella* made it necessary to design a new probe for this genus. This was done using the probe design tool in the ARB software package (29). The target position of DSU655 probe (655 to 673) was chosen to be in a highly accessible region according to Behrens et al. (6) and to be fully specific for the genus *Desulfurella* (checked with the ARB Probe Match tool). Using the described CARD-FISH protocol, the stringent hybridization conditions of *Desulfurella* probe were determined with positive-control cells of *Desulfurella kamchatkensis* and negative-control cells of *Syntrophobacter wolinii* (DSM 2805) and *Acidobacterium capsulatum* (DSM 11244) cultures. Hybridization stringency was optimized by increasing formamide concentrations starting with 10% in 5% steps. A 35% formamide concentration was optimal, resulting in high signal intensity of *D. kamchatkensis* and no signal for the negative controls.

SEM. Sediment samples were studied by scanning electron microscopy (SEM) as described elsewhere (2). Samples were fixed by immersion in glutaraldehyde (2.5%) for 2 h, washed twice in sodium cacodylate buf-

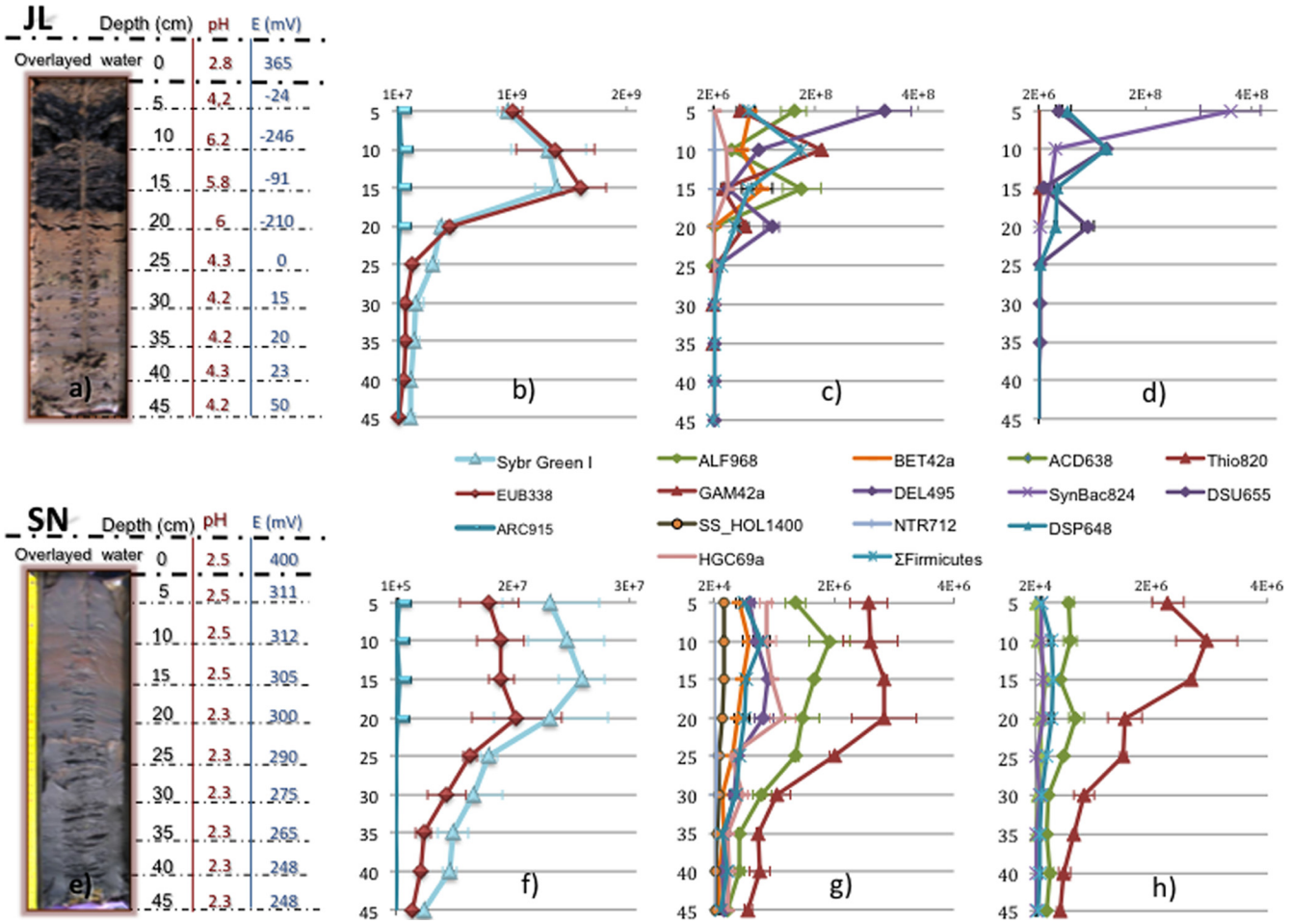

FIG 2 Depth profiles of pH and redox at JL (a) and *SN* (e), Sybr green I and domain-specific probes counts at JL (b) and SN (f), phylum-specific probes counts at JL (c) and SN (g), and genus-specific probes counts at JL (d) and SN (h).

fer (0.2 M, pH 7.1), and dehydrated in a graded series (10, 30, 50, 70, 90, and 100%) of ethanol-water mixtures for 20 min each. After dehydration, the samples were critical point dried and mounted on stubs. After gold shadowing, the samples were examined with a Phillips XL30 EDAX DX4i SEM.

RESULTS

Physicochemical properties of the sediments. The redox potential and pH values of the sediment profiles were significantly different (P value of <0.001 with the Mann-Whitney U test) at the two sites (JL and SN) (Fig. 2a and b). JL cores were banded and varied from reducing (blackish) to oxidizing (brownish) zones, with a redox ranging from −246 to 50 mV and a pH range from 6.2 to 4.2. SN cores did not show strong variations with depth, the pH remained between 2.3 and 2.5, and the redox potential remained between +248 and +312 mV.

Comparing the black and brown layers of the JL dam, arsenic, heavy metals, and sulfate concentrations in the interstitial water were higher in the brown layers. In the black layers, there was a strong decrease (higher than 90%) for Co, Ni, Cu, Zn, and As and close to 50% for Fe, Mn, and sulfate (Table 2). A concentration of 79 mg liter^{-1} of acetate, an intermediary of the anaerobic digestion pathways and a substrate for some methanogens and sulfate reducers, was measured in the black band, and the concentration in the brown band was as low as 1 mg l^{-1}. On the other hand, there was no stratification with depth at the SN dam, so the average of both studied layers is presented in Table 2. Compared to in JL, heavy metal concentrations varied strongly in SN: Co and Ni were under the detection limit, while the concentrations of Zn and Cu were much higher.

Chemistries of the overlaying waters at both dams were similar in pH and some metals (Table 3) but differed for K, Mn, Cd, P, S, and Fe. S and Fe are the elements that the oxidation of pyrite (the main substrate in the IPB) put into solution in ferric iron and sulfate forms. Both elements were less abundant at the JL dam, probably due to a dilution along the river of the concentrated ARD waters present at the SN dam.

Total cell counts with the Sybr green I method. In comparison to DAPI (4′,6-diamidino-2-phenylindole) staining, the use of the highly sensitive Sybr green I dye in combination with the Moviol embedding medium that lowered photobleaching and the use of black filters, which have less background, significantly improved the signal-to-noise ratio. This enabled reliable counting of total cell numbers.

The average of Sybr green I-stained cells of the JL core (Fig. 2b) was 5.5×10^8 cells g^{-1} wet weight of sediment, whereas in the SN dam sediments (Fig. 2f), the average was 1.4×10^7, which is 40-

TABLE 1 Oligonucleotide probes used in this study

Probe name	Sequence (5′ → 3′)	Target microorganism(s)	% FA[a]	Reference
NON338	ACTCCTACGGGAGGCAGC		0	47
EUB338	GCTGCCTCCCGTAGGAGT	*Bacteria*	35	3
EUB338-II	GCAGCCACCCGTAGGTGT	*Planctomyces*	35	9
EUB338-III	GCTGCCACCCGTAGGTGT	*Verrucomicrobiae* (and others)	35	9
ALF968	GGTAAGGTTCTGCGCGTT	*Alphaproteobacteria*, except of *Rickettsiales*	20	35
ACD840	CGACACTGAAGTGCTAAGC	*Acidiphilium* spp.	10	12
BET42a[b]	GCCTTCCCACTTCGTTT	*Betaproteobacteria*	35	32
GAM42a[c]	GCCTTCCCACATCGTTT	*Gammaproteobacteria*	35	32
THIO820	ACCAAACATCTAGTATTCATCG	*Acidithiobacillus* spp.	10	37
DELTA495a	AGTTAGCCGGTGCTTCCT	Most *Deltaproteobacteria* and *Gemmatimonadetes*	30	27
cDELTA495a	AGTTAGCCGGTGCTTCTT	Competitor for DEL495a		31
DELTA495b	AGT TAG CCG GCG CTTCCT	Some *Deltaproteobacteria*	30	27
cDELTA495b	AGTTAGCCGGCGCTTC(T/G)T	Competitor for DEL495b		28
DELTA495c	AATTAGCCGGTGCTTCCT	Some *Deltaproteobacteria*	30	27
cDELTA495c	AATTAGCCGGTGCTTCTT	Competitor for DEL495c		28
SYNBAC824	GTACCCGCTACACCTAGT	*Syntrophobacter* spp.	10	4
DSU655	CGCTTGCTTTTCCCGAAC	*Desulfurella* spp.	35	This study
HGC69a	TATAGTTACCACCGCCGT	Gram-positive high GC content (*Actinobacteria*)	25	40
ARCH915	GTGCTCCCCCGCCAATTCCT	*Archaea*	35	45
LGC354a	TGGAAGATTCCCTACTGC	Gram-positive low GC DNA content (*Firmicutes*)	35	33
LGC354b	CGGAAGATTCCCTACTGC	Gram-positive low GC DNA content (*Firmicutes*)	35	33
CLIT135	GTTATCCGTGTGTACAGGG	*Clostridium* cluster XI	0	15
CLOST1	TTCTTCCTAATCTCTACGCA	*Clostridium* clusters I and II	30	24
NTR712	CGCCTTCGCCACCGGCCTTCC	*Nitrospira* group	35	10
NTR712c	CGCCTTCGCCACCGGTGTTCC	Competitor for NTR712		10
DSP648	CTCTCCTGTCCTCAAGAT	*Desulfosporosinus*, *Desulfitobacterium*, *Dehalobacter* spp.	30	18
SS_HOL1400	TTCGTGATGTGACGGGC	*Acidobacteria*	20	34
EUK516	ACCAGACTTGCCCTCC	*Eukarya*	30	3

[a] Formamide concentration in the hybridization buffer to ensure specific detection of target organisms.
[b] Used with unlabeled GAM42a as competitor.
[c] Used with unlabeled BET42a as competitor.

fold lower. A common feature among depth profiles of both sites is that cell numbers in both dams are higher in the 15-to-20-cm layer. After that, depth profiles followed a general trend observed in many sediments of a drastic decrease with depth (25), from 1.4×10^9 cells g^{-1} (wet weight) in the 15-to-20-cm layer to 1.3×10^8 in the 25-to-30-cm layer in the JL dam (10-fold lower) and from 2.4×10^7 to 3.7×10^6 in the SN dam (6-fold lower).

SEM. Scanning electron microscopy (SEM) analysis of sediments revealed high densities of cells attached to the sediment particles in the black layer of site JL. The colonization of the brownish layer of JL and of sediment from site SN was scarce. This corroborated the direct counts obtained with the Sybr green I method.

CARD-FISH. The sites investigated here had already been characterized in an earlier study by comparative 16S rRNA gene analysis, applying both fingerprinting by DGGE and comparative sequence analysis (42). FISH-based quantifications of particular taxa had first been hampered by high background due to the autofluorescence of sediment particles. These problems were solved in this study by applying the improved whole-cell hybridization technique CARD-FISH enabling the quantification of higher and lower taxa in a nested approach.

(i) Domain-specific probes. First, oligonucleotide probes for the domains *Bacteria*, *Archaea*, and *Eukarya* were applied to the sediment samples. In all cases, *Bacteria* (>98%) dominated over *Archaea* (<2%) and *Eukarya* (below the detection limit) (Fig. 2b and f). As for the Sybr green I total cell counts, great differences were found between the two sampling sites. In the JL sediment, the average bacterial counts with probes EUB338 I to III (Fig. 2b) was 5.4×10^8 cells g^{-1} (wet weight) of sediment, ranging from 1.61×10^9 at 15 cm to 2.12×10^7 at 45 cm, whereas in the SN dam (Fig. 2f), the average was 8.9×10^6, ranging from 1.6×10^7 at 15 cm to 2.2×10^6 at 45 cm.

(ii) In-depth analysis of the bacterial community. An earlier study of Tinto sediments (42) had retrieved sequences belonging to five phyla of the domain *Bacteria*: *Proteobacteria* of the classes *Alpha-*, *Beta-*, *Gamma-*, and *Deltaproteobacteria*; *Acidobacteria*; *Nitrospira*; *Actinobacteria*; and *Firmicutes*. The selection of the phylum- and class-specific probes used in this study was done according to these previous findings.

Depth profiles of the respective bacterial groups are shown in Fig. 2c and g. In JL dam sediments, *Deltaproteobacteria* was the most abundant group along the sediment core, as detected by probe DEL495a-c (average of 6.6×10^7 cells g^{-1} [wet weight]). This class of *Proteobacteria* showed a strong variation with depth with two population maxima. The first peak (3.3×10^8 cells g^{-1} [wet weight]) was detected within the uppermost 5 cm, and after a sharp decline, a second population maximum (1.1×10^8 cells g^{-1} [wet weight]) was found in the most reduced layer (15 to 20 cm). The second most abundant group was *Firmicutes*, detected with a probe mix consisting of LGC354a, LGC354b, CLIT135, CLOSTI, and DSP648, with an average along the profile of 4.3×10^7 cells g^{-1} (wet weight). *Alphaproteobacteria* as detected by probe ALF968 averaged 4.2×10^7 cells g^{-1} (wet weight), *Gammaproteo-*

TABLE 2 Heavy metals, metaloids, sulfate, and volatile fatty acid concentrations detected in the porewater sediments and percentage of reduction in JL layers

Sample	Concn (mM)[a]											
	Formate	Acetate	Sulfate	Fe	Co	Ni	Cu	Zn	As	Al	Mn
SN	$1.1 \times 10^{-2} \pm 2.1 \times 10^{-3}$	$0.1 \pm 2.1 \times 10^{-2}$	20.4 ± 2.3	92.2 ± 2.1	UDL	UDL	1.0 ± 0.2	11.2 ± 0.4	$1.1 \times 10^{-2} \pm 9 \times 10^{-4}$	43 ± 3.5	2.9 ± 0.2
JL brown	$1.3 \times 10^{-2} \pm 3.2 \times 10^{-3}$	$6.6 \times 10^{-3} \pm 3.2 \times 10^{-4}$	25.5 ± 3.1	100.2 ± 1.2	$1.3 \times 10^{-1} \pm 5 \times 10^{-3}$	$4.4 \times 10^{-2} \pm 8 \times 10^{-4}$	$7.9 \times 10^{-3} \pm 3 \times 10^{-4}$	1.9 ± 0.1	$1.4 \times 10^{-2} \pm 2.5 \times 10^{-3}$	33 ± 1.4	4.1 ± 1.4
JL black	$1.1 \times 10^{-2} \pm 2.1 \times 10^{-3}$	$1.3 \pm 1.5 \times 10^{-2}$	12.5 ± 1	52.2 ± 3.3	$1.2 \times 10^{-2} \pm 2.1 \times 10^{-3}$	$1 \times 10^{-3} \pm 2.4 \times 10^{-4}$	$3.1 \times 10^{-4} \pm 1 \times 10^{-5}$	$6.1 \times 10^{-3} \pm 4.1 \times 10^{-4}$	$1.3 \times 10^{-3} \pm 4.5 \times 10^{-4}$	$3.3 \times 10^{-2} \pm 4 \times 10^{-3}$	2.1 ± 0.1
% reduction in JL black			51.1	47.9	90.9	97.7	96.0	99.7	90.6	99.9	48.3

[a] UDL, under the detection limit.

bacteria as detected by probe GAM42a averaged 4.0×10^7 cells g^{-1} (wet weight), and *Betaproteobacteria* as detected with probe BET42a averaged 2.6×10^7 cells g^{-1} (wet weight). In contrast, *Acidobacteria* (SS_HOL1400 probe) and *Actinomicetales* (HGC69a probe) appeared only in low numbers, 5.9×10^5 and 7.7×10^6 cells g^{-1} (wet weight), respectively. Signals for probe NTR712 (*Nitrospira* group) were below the detection limit.

The depth profiles of SN dam sediments did not show the variation found in JL. In this core, numbers decrease homogeneously with depth. *Gammaproteobacteria* dominated (average 1.7×10^6 cells g^{-1} [wet weight]) followed by *Alphaproteobacteria* with an average along the profile of 1.1×10^6 cells g^{-1} (wet weight). The rest of the groups were close to the detection limit, around 10^5 cells g^{-1} (wet weight), in decreasing order: *Actinomycetales*, *Deltaproteobacteria*, *Firmicutes*, *Betaproteobacteria*, and *Acidobacteria*.

(iii) Genus-specific probes. All genus-specific probes applied in this study were targeting genera for which sequences had been frequently retrieved in an earlier study (42). This included the deltaproteobacterial genera *Syntrophobacter* (probe Synbac824) and *Desulfurella* (probe DSU655), the genus *Desulfosporosinus* (probe DSP648) within the phylum *Firmicutes*, the alphaproteobacterial genus *Acidiphilium* (probe ACD638), and the gammaproteobactrial genus *Acidithiobacillus* (Thio820).

The genus-specific probing confirmed the great differences between the two sampling sites (Fig. 2d and h). In JL, the most abundant genus detected was *Syntrophobacter*. Cells were rod-shaped and had a size of about 2 by 1 μm. The average along the profile was 4.7×10^7 cells g^{-1} (wet weight), but just in the first layer the signal counts were 3.6×10^8, representing 36% of the total *Bacteria* counts. *Syntrophobacter* spp. are propionate-degrading syntrophic bacteria that use sulfate as the electron acceptor. They typically occur in environments with neutral pH. The other abundant genera were *Desulfurella* (3.1×10^7 cells g^{-1} [wet weight], mostly rods of a size of 2 by 1 μm), and *Desulfosporosinus* (2.8×10^7 cells g^{-1} [wet weight], curved rods of a size of 2 to 4 by 0.7 μm). The latter genus is known to encompass spore-forming sulfate-reducing bacteria. Both genera showed higher numbers at those layers with higher pH and reducing redox potential (5 to 10 and 15 to 20 cm) (Fig. 2a and d). At SN, *Acidithiobacillus* spp. dominated with an average of 1.5×10^6 cells g^{-1} (wet weight) along the profile. The hybridized cells were coccoid rods with a size of 1 by 0.7 μm. *Acidithiobacillus* spp. derive energy from the oxidation of reduced sulfur compound and/or ferrous iron, or the reduction of ferric iron under anoxic conditions. Finally, *Acidiphilium* spp. were also present, with average numbers of 4.2×10^5 cells g^{-1} (wet weight) (rods of a size of 2 to 3 by 1 μm).

DISCUSSION

We used a nested-probe approach for the quantification of the microbial community composition in sediments of Tinto River. The generally low abundance of *Archaea* agreed with similar results found in the sediments of mine tailing dumps (23). In a previous study of Río Tinto sediments (42), the archaeal diversity had been restricted to two genera: *Ferroplasma* spp. and *Thermoplasma* spp. Although Sanz et al. (43) had described the presence of methanogens in the sediments of the Tinto basin, our data suggest that *Archaea* play a minor role in the ecology of these sediments. Both *Ferroplasma* and *Thermoplasma* are usually found in bioleaching operations at lower pH (around 2) and at

much higher iron and sulfate concentrations than those prevailing in Río Tinto sediments (13). Although algae, ciliates, flagellates, amoebae, and fungi have been reported in the water column and the biofilms of the Río Tinto (1, 5), no *Eukarya* probe signal was detected by CARD-FISH; therefore, *Bacteria* seem to fully dominate the anoxic sediment layers of Tinto River.

When genus-specific probes were applied, a pronounced variability was detected between the two sampling sites. In SN sediments, where parameters such as pH and redox potential were similar to water column values, *Bacteria* related to the iron cycle prevailed, likely reflecting the higher availability of iron at low pH and oxidative redox potential. This included the genera *Acidiphilium* (ACD638 probe) and *Acidithiobacillus* (Thio820 probe), which both are capable of iron reduction under anoxic conditions. No members of the *Leptospirillum* genus, *Nitrospira*-like bacteria (Ntr712 probe), were detected. The common iron oxidizers in ARD environments are members of the aerobic genus *Leptospirillum* and the facultative anaerobe bacterium *Acidithiobacillus ferrooxidans*, which can oxidize iron and sulfur in aerobic conditions and reduce iron in anoxia. Our results confirm the dominance of the versatile *Acidithiobacillus ferrooxidans* in the sediments over the strictly aerobic *Leptospirillum* spp. that usually dominate in extremely acidic oxic ARD environments (7, 13).

At the JL dam, where the iron solubility is lower due to higher pH and reducing redox potential, microbes of the sulfur cycle were most abundant. Here, sulfate-reducing bacteria (SRB) of the genera *Desulfosporosinus* (DSP 648 probe) and *Syntrophobacter* (Syn824 probe) as well as sulfur reducers of the genus *Desulfurella* (DSU655 probe) predominated, showing the importance of sulfur cycling in these sediments. *Syntrophobacter*-affiliated 16S rRNA gene sequences (42) (HQ730668, HQ730666) have been retrieved in several acidic environments before (11, 17, 26), suggesting that not-yet-cultured relatives of *Syntrophobacter* might be well adapted to acidic conditions in contrast to the general neutral pH environments where they thrive.

The analyses of both brown and black layers in the JL sediments showed a significant reduction in the last ones for dissolved metals, iron, and sulfate in the black layers, which run parallel to the SRB abundance. *Desulfurella* and *Desulfosporosinus* abundance peaked perfectly with those black layers where the pH values and acetate concentration increased and the redox potential and the levels of the sulfate and the dissolved metals decreased. Our results suggest that the attenuation of ARD characteristics in the reduced black layers is biologically driven by SRB. The dissimilative reduction of sulfate, driven by identified sulfate- and sulfur-reducing bacteria, leads to a consumption of protons, thus increasing alkalinity, and to sulfide formation. In addition, there is a sulfide-mediated metal precipitation: the sulfide reacts with the dissolved iron and other heavy metals which can form black amorphous precipitates (FeS) and metallic sulfides (MS). These results agree with previous studies where remediation in AMD associated with SRB metabolism was observed (14, 16, 21, 39).

In summary, the CARD-FISH quantifications performed in this study underline the great differences between microbial communities of the two Río Tinto sediments studied that had been previously indicated by DGGE and comparative sequence analysis. These differences correlate with their physicochemical characteristics, which would correspond to different hydrology at both sites. In the JL dam, the location, thickness, and values of pH and redox potential of the oxidized and reduced zones vary tempo-

TABLE 3 Element concentration, TOC, redox potential, and pH values of SN and JL overlaid waters

Sample	pH	E (mV)	TOC (mg l^{-1})	Concn (mM)[a]												
				Na	Mg	Al	K	Mn	Fe	Cu	Zn	As	Ca	Cd	S	P
SN	2.5	400	9 ± 1.7	0.62 ± 0.1	8.3 ± 0.3	14.5 ± 0.7	0.23 ± 0.01	UDL	41.30 ± 2.4	0.43 ± 0.04	1.19 ± 0.3	$0.07 \pm 2.1 \times 10^{-3}$	1.81 ± 0.07	$2.7 \times 10^{-3} \pm 8 \times 10^{-4}$	85.8 ± 6.4	2.3 ± 0.7
JL	2.8	365	20 ± 4	0.24 ± 0.02	12.3 ± 0.4	13.6 ± 0.4	UDL	26.07 ± 1.3	16.34 ± 1.7	1.94 ± 0.07	1.41 ± 0.05	$0.04 \pm 3.7 \times 10^{-3}$	0.98 ± 0.05	UDL	54.3 ± 4.6	UDL

[a] UDL, under the detection limit.

rally, but stratification has been routinely observed. In contrast, sediments in SN have been more homogeneous. Different interpretations can be put forward. On the one hand, the two sampling sites have different hydrology. Site SN is a stream located close to the source of the river with a constant water flow containing a high concentration of heavy metals, mainly iron. Therefore, the sediment characteristics are close to those of the water column strongly buffered by ferric iron. In contrast, the site JL is located 5 km downstream, with an increasing flow due to the addition of neutral tributaries which lower the iron concentration, albeit with a strong seasonal variability. One of the tributaries upstream of JL contains the waters from the municipal wastewater treatment plant of Nerva. This significantly increases the total organic content (TOC) of the waters. The combination of both factors could explain the differences detected in both types of sediments. At the JL dam, with seasonal variability, higher TOC, and lower iron concentration, microbial reduction processes such as sulfate reduction increase the pH. This effect would take place firstly in microniches and then expands to macroscopic conditions. That would explain the banded sediment at the JL dam, which would correspond to the fluctuating conditions of the input water. Within them, SRB communities reduce the dissolved sulfates to sulfides that precipitate iron and heavy metals, performing a local natural bioremediation of Tinto River.

ACKNOWLEDGMENTS

This research was supported by the Spanish "Ministerio de Ciencia e Innovación" grant CTM2009-10521 to J.L. Sanz and grant CGL2009-11059 to R. Amils and by the Max Planck Society. Irene Sánchez-Andrea is a predoctoral fellowship of the same agency.

We thank Nuria Rodríguez for her help with the fieldwork, Sara Kleindienst and Kyoko Kubo for their help introducing the CARD-FISH technique, and Ana Suárez for her invaluable help with the ARB program.

REFERENCES

1. **Aguilera A, Manrubia SC, Gomez F, Rodriguez N, Amils R.** 2006. Eukaryotic community distribution and its relationship to water physicochemical parameters in an extreme acidic environment, Rio Tinto (Southwestern Spain). Appl. Environ. Microbiol. **72**:5325–5330.
2. **Alphenaar PA, Groeneveld N, Van Aelst AC.** 1994. Scanning electron microscopical method for internal structure analysis of anaerobic granular sludge. Micron **25**:129–133.
3. **Amann RI, et al.** 1990. Combination of 16S rRNA-targeted oligonucleotide probes with flow cytometry for analyzing mixed microbial populations. Appl. Environ. Microbiol. **56**:1919–1925.
4. **Ariesyady HD, Ito T, Yoshiguchi K, Okabe S.** 2007. Phylogenetic and functional diversity of propionate-oxidizing bacteria in an anaerobic digester sludge. Appl. Microbiol. Biotechnol. **75**:673–683.
5. **Baker BJ, Tyson GW, Goosherst L, Banfield JF.** 2009. Insights into the diversity of eukaryotes in acid mine drainage biofilm communities. Appl. Environ. Microbiol. **75**:2192–2199.
6. **Behrens S, et al.** 2003. In situ accessibility of small-subunit rRNA of members of the domains *Bacteria*, *Archaea*, and *Eucarya* to Cy3-labeled oligonucleotide probes. Appl. Environ. Microbiol. **69**:1748–1758.
7. **Bond PL, Druschel GK, Banfield JF.** 2000. Comparison of acid mine drainage microbial communities in physically and geochemically distinct ecosystems. Appl. Environ. Microbiol. **66**:4962–4971.
8. **Bruneel O, Duran R, Casiot C, Elbaz-Poulichet F, Personné JC.** 2006. Diversity of microorganisms in Fe-As-rich acid mine drainage waters of Carnoules, France. Appl. Environ. Microbiol. **72**:551–556.
9. **Daims H, Brühl A, Amann R, Schleifer KH, Wagner M.** 1999. The domain-specific probe EUB 338 is insufficient for the detection of all bacteria: development and evaluation of a more comprehensive probe set. Syst. Appl. Microbiol. **22**:434–444.
10. **Daims H, Nielsen JL, Nielsen PH, Schleifer KH, Wagner M.** 2001. In situ characterization of *Nitrospira*-like nitrite-oxidizing bacteria active in wastewater treatment plants. Appl. Environ. Microbiol. **67**:5273–5284.
11. **Dedysh SN, Pankratov TA, Belova SE, Kulichevskaya IS, Liesack W.** 2006. Phylogenetic analysis and in situ identification of *Bacteria* community composition in an acidic *Sphagnum* peat bog. Appl. Environ. Microbiol. **72**:2110–2117.
12. **Demanèche S, et al.** 2008. Antibiotic-resistant soil bacteria in transgenic plant fields. Proc. Nat. Acad. Sci. **105**:3957–3962.
13. **Edwards KJ, Gihring TM, Banfield JF.** 1999. Seasonal variations in microbial populations and environmental conditions in an extreme acid mine drainage environment. Appl. Environ. Microbiol. **65**:3627–3632.
14. **Fortin D, Rioux JP, Roy M.** 2002. Geochemistry of iron and sulfur in the zone of microbial sulfate reduction in mine tailings. Water Air Soil Poll. **2**:37–56.
15. **Franks AH, et al.** 1998. Variations of bacterial populations in human feces measured by fluorescent in situ hybridization with group-specific 16S rRNA-targeted oligonucleotide probes. Appl. Environ. Microbiol. **64**: 3336–3345.
16. **Friese K, et al.** 1998. Biogeochemistry of iron and sulfur in sediments of an acidic mining lake in Lusatia, Germany. Water Air Soil Poll. **108**:231–247.

16a. **Garcia-Moyano A, Gonzalez-Toris E, Aguilera A, Amils R.** 2007. Prokaryotic community composition and ecology of floating macroscopic filaments from an extreme acidic environment, Rio Tinto (SW, Spain). Syst. Appl. Microbiol. **30**:601–614.

17. **Gonzalez-Toril E, et al.** 2011. Geomicrobiology of La Zarza-Perrunal acid mine effluent (Iberian Pyritic Belt, Spain). Appl. Environ. Microbiol. **77**: 2685–2694.
18. **González-Toril E, Gómez F, Malki M, Amils R.** 2006. The isolation and study of acidophilic microorganisms, p 471–510. *In* Rainey FA, Oren A (ed), Extremophiles—methods in microbiology. Elsevier/Academic Press, London, United Kingdom.
19. **Gonzalez-Toril E, Llobet-Brossa E, Casamayor EO, Amann R, Amils R.** 2003. Microbial ecology of an extreme acidic environment, the Tinto River. Appl. Environ. Microbiol. **69**:4853–4865.
20. **Johnson DB.** 1998. Biodiversity and ecology of acidophilic microorganisms. FEMS Microbiol. Ecol. **27**:307–317.
21. **Johnson DB, Hallberg KB.** 2005. Acid mine drainage remediation options: a review. Sci. Total Environ. **338**:3–14.
22. **Johnson DB, Hallberg KB.** 2009. Carbon, iron and sulfur metabolism in acidophilic micro-organisms. Adv. Microb. Physiol. **54**:201–255.
23. **Kock D, Schippers A.** 2008. Quantitative microbial community analysis of three different sulfidic mine tailing dumps generating acid mine drainage. Appl. Environ. Microbiol. **74**:5211–5219.
24. **Kusel K, Pinkart HC, Drake HL, Devereux R.** 1999. Acetogenic and sulfate-reducing bacteria inhabiting the rhizoplane and deep cortex cells of the sea grass *Halodule wrightii.* Appl. Environ. Microbiol. **65**:5117–5123.
25. **Llobet-Brossa E, Rosselló-Mora R, Amann R.** 1998. Microbial community composition of Wadden Sea sediments as revealed by fluorescence *in situ* hybridization. Appl. Environ. Microbiol. **64**:2691–2696.
26. **Loy A, Kusel K, Lehner A, Drake HL, Wagner M.** 2004. Microarray and functional gene analyses of sulfate-reducing prokaryotes in low-sulfate, acidic fens reveal cooccurrence of recognized genera and novel lineages. Appl. Environ. Microbiol. **70**:6998–7009.
27. **Loy A, et al.** 2002. Oligonucleotide microarray for 16S rRNA gene-based detection of all recognized lineages of sulfate-reducing prokaryotes in the environment. Appl. Environ. Microbiol. **68**:5064–5081.
28. **Lücker S, et al.** 2007. Improved 16S rRNA-targeted probe set for analysis of sulfate-reducing bacteria by fluorescence *in situ* hybridization. J. Microbiol. Methods **69**:523–528.
29. **Ludwig W, Strunk O, Westram R, Richter L, Meier H.** 2004. ARB: a software environment for sequence data. Nucleic Acids Res. **32**:1363–1371.
30. **Lunau M, Lemke A, Walther K, Martens-Habbena W, Simon M.** 2005. An improved method for counting bacteria from sediments and turbid environments by epifluorescence microscopy. Environ. Microbiol. **7**:961–968.
31. **Macalady JL, et al.** 2006. Dominant microbial populations in limestone-corroding stream biofilms, Frasassi cave system, Italy. Appl. Environ. Microbiol. **72**:5596–5609.
32. **Manz W, Amann R, Ludwig W, Wagner M, Schleifer KH.** 1992. Phy-

logenetic oligodeoxynucleotide probes for the major subclasses of proteobacteria: problems and solutions. Syst. Appl. Microbiol. **15**:593–600.
33. **Meier H, Amann R, Ludwig W, Schleifer KH.** 1999. Specific oligonucleotide probes for *in situ* detection of a major group of Gram-positive bacteria with low DNA G+C content. Syst. Appl. Microbiol. **22**:186–196.
34. **Meisinger DB, et al.** 2007. *In situ* detection of novel *Acidobacteria* in microbial mats from a chemolithoautotrophically based cave ecosystem (Lower Kane Cave, WY, U.S.A.). Environ. Microbiol. **9**:1523–1534.
35. **Neef A.** 1997. Anwendung der in situ Einzelzell-Identifizierung von Bakterien zur Populationsanalyse in komplexen mikrobiellen Biozönosen. Technische Universität München, Munich, Germany.
36. **Nordstrom DK, Alpers CN.** 1999. Negative pH, efflorescent mineralogy, and consequences for environmental restoration at the Iron Mountain Superfund site, California. Proc. Natl. Acad. Sci. U. S. A. **96**:3455–3462.
37. **Peccia J, Marchand EA, Silverstein J, Hernandez M.** 2000. Development and application of small-subunit rRNA probes for assessment of selected *Thiobacillus* species and members of the genus *Acidiphilium.* Appl. Environ. Microbiol. **66**:3065–3072.
38. **Pernthaler A, Pernthaler J, Amann R.** 2002. Fluorescence *in situ* hybridization and catalyzed reporter deposition for the identification of marine bacteria. Appl. Environ. Microbiol. **68**:3094–3101.
39. **Praharaj T, Fortin D.** 2004. Indicators of microbial sulfate reduction in acidic sulfide-rich mine tailings. Geomicrobiol. J. **21**:457–467.
40. **Roller C, Wagner M, Amann R, Ludwig W, Schleifer KH.** 1994. *In situ* probing of Gram-positive bacteria with high DNA G+C content using 23S rRNA-targeted oligonucleotides. Microbiology **140**:2849–2858.
41. **Rowe OF, JSánchez-España Hallberg KB, Johnson DB.** 2007. Microbial communities and geochemical dynamics in an extremely acidic, metal-rich stream at an abandoned sulfide mine (Huelva, Spain) underpinned by two functional primary production systems. Environ. Microbiol. **9**:1761–1771.
42. **Sánchez-Andrea I, Rodriguez N, Amils R, Sanz JL.** 2011. Microbial diversity in anaerobic sediments at Rio Tinto, a naturally acidic environment with a high heavy metal content. Appl. Environ. Microbiol. **77**:6085–6093.
43. **Sanz JL, Rodríguez N, Díaz EE, Amils R.** 2011. Methanogenesis in the sediments of Rio Tinto, an extreme acidic river. Environ. Microbiol. **13**:2336–2341.
44. **Sekar R, et al.** 2003. An improved protocol for quantification of freshwater *Actinobacteria* by fluorescence *in situ* hybridization. Appl. Environ. Microbiol. **69**:2928–2935.
45. **Stahl DA, Amann R.** 1991. Development and application of nucleic acid probes, p 205–248. *In* Stackebrandt E, Goodfellow M (ed), Nucleic acid techniques in bacterial systematics. John Wiley & Sons, Ltd., Chichester, United Kingdom.
46. **Teira E, Reinthaler T, Pernthaler A, Pernthaler J, Herndl GJ.** 2004. Combining catalyzed reporter deposition-fluorescence *in situ* hybridization and microautoradiography to detect substrate utilization by bacteria and archaea in the deep ocean. Appl. Environ. Microbiol. **70**:4411–4414.
47. **Wallner G, Amann R, Beisker W.** 1993. Optimizing fluorescent *in situ* hybridization with rRNA-targeted oligonucleotide probes for flow cytometric identification of microorganisms. Cytometry **14**:136–143.
48. **Whiteley AS, Griffiths RI, Bailey MJ.** 2003. Analysis of the microbial functional diversity within water-stressed soil communities by flow cytometric analysis and CTC+ cell sorting. J. Microbiol. Methods **54**:257–267.